Available online at www.sciencedirect.com
SCIENCE DIRECT
Journal of Catalysis 238 (2006) 260–269
JOURNAL OF CATALYSIS
www.elsevier.com/locate/jcat

Combined in situ XPS and PTRMS study of ethylene epoxidation over silver

Valerii I. Bukhtiyarov [a,*], Alexander I. Nizovskii [a], Hendrik Bluhm [b,1], Michael Hävecker [b], Evgueni Kleimenov [b], Axel Knop-Gericke [b], Robert Schlögl [b]

[a] *Boreskov Institute of Catalysis, Lavrentieva ave. 5, Novosibirsk, 630090, Russia*
[b] *Fritz-Haber-Institut der MPG, Faradayweg 4-6, Dahlem, Berlin, Germany*

Received 31 March 2005; revised 5 November 2005; accepted 21 November 2005

Available online 18 January 2006

Abstract

Ethylene epoxidation over silver was investigated by combined in situ X-ray photoelectron spectroscopy (XPS) and proton-transfer reaction mass spectrometry (PTRMS) at 300–520 K and 0.07–1 mbar. Ethylene oxide was present among the reaction products at $T \geqslant 420$ K and $p \geqslant 0.3$ mbar. The catalytically active surface contains two oxygen species – nucleophilic and electrophilic oxygen. The observed correlation between the abundance of electrophilic oxygen and the yield of ethylene oxide expressed as C_2H_4O partial pressure indicates that namely this oxygen species oxidizes ethylene to ethylene oxide. Opposite trend is observed for nucleophilic oxygen: the higher is the abundance of this species, the lower is the yield of ethylene oxide. This result is in line with the known fact that because of its oxidic nature, nucleophilic oxygen is active in total oxidation of ethylene to CO_2 and H_2O. The low activity of silver at $T < 420$ K is caused by the presence of carbonates and carbonaceous residues at the silver surface that reduce the available silver surface area for the catalytic reaction. Reduction of the surface area available for the formation of active species due to accumulation of the embedded oxygen species also explains the decreased rate of ethylene oxide formation with time observed for $T \geqslant 470$ K.

Keywords: Silver; Catalyst; Oxygen; Ethylene; Epoxidation; In situ XPS; PTRMS

1. Introduction

The relationship between the structure of a catalyst and its catalytic activity has motivated many investigations that have applied surface-sensitive methods to study heterogeneous catalytic systems. These experiments focused on the chemical composition and morphology of catalyst surfaces, the nature of adsorbed species, and reaction intermediates. Most of these studies were performed ex situ (i.e., not in the presence of the reaction gas mixture), and a priori transfer of the results of these studies to technical catalysis is difficult because of the pressure gap problem. The evacuation of the reaction gas mixtures, which is a usual step in postreaction analysis, can lead to the destruction of the active centers on the catalyst surface due to the removal of, say, weakly bound species or a change in the chemical nature of the surface constituents. Consequently, catalyst surfaces under operating catalytic conditions ($p > 1$ mbar) can be quite different from those same surfaces under high vacuum conditions ($p < 10^{-6}$ mbar).

In the past, silver catalysts for ethylene epoxidation have been studied mostly under ex situ conditions with high-vacuum-based surface science techniques [1–8]. Our own previous studies were also not free from this drawback [9,10]. Due in part to the absence of real in situ investigations, the exact mechanism of this reaction is still under debate. Two primary aspects are under discussion: the nature of the epoxidizing oxygen [1–4] and the nature of the key intermediate that leads to the formation of ethylene oxide. Both oxametallacycle [11,12] and π-bonded ethylene [3,8,13] are discussed in the literature, but on the basis of the currently available data, it is difficult to determine which species is indeed the intermediate in the epoxidation route, or whether both species serve this purpose. Recent microkinetic modeling investigations [14,15] elucidated

* Corresponding author.
E-mail address: vib@catalysis.ru (V.I. Bukhtiyarov).
[1] Present address: Lawrence Berkeley National Laboratory, Chemical Sciences Division, Berkeley, CA 94720, USA.

0021-9517/$ – see front matter
doi:10.1016/j.jcat.2005.11.043

some aspects of the reaction mechanism; however, experimental studies under in situ conditions, which can provide a direct correlation between the catalytic activity and the surface composition, have not been reported to date.

In recent years, a number of techniques have been adapted to operate under reaction conditions (>0.1 mbar), including X-ray absorption spectroscopy (XAS) [16,17], sum frequency generation (SFG) [18,19], infrared absorption spectroscopy (IRAS) [20,21], and scanning tunneling microscopy (STM) [22,23]. However, in most cases the application of these techniques to catalytic systems have not been considered actual in situ studies, because catalytic performance cannot be measured simultaneously with an analysis of the catalyst surface. This makes it difficult to correlate the nature of the species adsorbed on a catalyst surface with its catalytic activity and/or selectivity. Consequently, the surface species observed even at elevated pressures cannot be directly attributed to catalytically active species.

In this paper we present the results of simultaneously performed in situ X-ray photoelectron spectroscopy (XPS) and proton-transfer reaction mass spectrometry (PTRMS) experiments of ethylene epoxidation over silver. Because of its versatility and sensitivity to the chemical state of an element, XPS is one of the most powerful methods for studying the surface of heterogeneous catalysts. In situ XPS has been used in the past to study catalysts under reaction conditions at pressures of up to 2 mbar [24–29]. We have measured the yield of ethylene oxide using PTRMS, a detailed description of which has been given previously [30]. In brief, the ionization of gas-phase molecules for the subsequent mass spectrometric analysis proceeds through the transfer of protons from H_3O^+ ions, which are generated in a special source, to the analyzed substance. As a result, the method deals with a molecular ion, which has greater mass (plus one proton) than the ion in the routine mass spectrometric analysis. Only those ions with a higher proton affinity than H_2O will contribute to the PTRMS spectrum. This ionization method does cause less fragmentation of the analyzed molecules, simplifying the analysis of mass spectra. Another advantage of PTRMS is its high sensitivity to organic molecules, such as ethylene and ethylene oxide.

We have studied ethylene epoxidation over silver in the temperature range 300–520 K and under varying total pressures and ethylene-to-oxygen mixing ratios. Our combined PTRMS and in situ XPS experiments demonstrate that the composition of the oxygen overlayer on a silver surface correlates with the yield of ethylene oxide. Based on these data, we propose a reaction mechanism for the ethylene epoxidation over silver.

2. Experimental

The experiments were performed at beamline U49/2-PGM1 at BESSY in Berlin [31]. The prototype of the XPS instrument was described previously [28,29]. The key feature of this apparatus is an electrostatic lens system that focuses the electrons emitted by the sample (at a pressure of up to several mbar) into the focal plane of a hemispherical analyzer, which is situated downstream in the high-vacuum region. The overall spectral resolution in our measurements was better than 0.3 eV, as calibrated by Ar 2p gas-phase spectra. All spectra were normalized to the incident photon flux, which was measured with a photodiode of known quantum efficiency. The binding energies were calibrated against the Fermi edge of the sample. The incident photon energies in the measurements were 850 eV for O 1s, 700 eV for Ag 3d, and 610 eV for C 1s, which resulted in similar electron kinetic energies of ∼225 eV and thus similar probing depths in the O 1s, Ag 3d, and C 1s measurements. These kinetic energies correspond to inelastic mean free path lengths of the photoelectrons in a solid of about 10 Å. Because the electrons were detected under an angle of 55° to the surface normal, the effective probing depth was even smaller in our experiments.

The ethylene and oxygen flows into the experimental cell were regulated with calibrated mass flow controllers. The overall ethylene and oxygen pressure in the experimental cell was varied from 0.071 to 1.05 mbar, and the ratio of C_2H_4 to O_2 partial pressures was varied from about 1:10 to 1:1. Mass spectra were measured using a PTRMS produced by Ionicon Analytik (Austria). The ethylene pressure was monitored at $m/z = 29$ (C_2H_4 plus H^+), whereas the ethylene oxide pressure was monitored at $m/z = 45$ (C_2H_4O plus H^+). Because of its low proton affinity, CO_2 did not contribute to the PTRMS signal at $m/z = 45$. This was confirmed by the absence of a PTRMS signal at $m/z = 45$ in a blank experiment when 0.1 mbar CO_2 was admitted to the gas cell. Consequently, carbon dioxide was not measured in our experiments.

Because in our setup the PTRMS is connected to the reaction chamber via a capillary and a leak valve, leading to an essential drop in pressure between the reaction cell and the mass spectrometer, PTRMS signals measured experimentally reflect the concentrations of gas-phase molecules inside the mass spectrometer, but not in the reaction volume. Moreover, the gas flow to the PTRMS was regulated by a leak valve, which was necessary to avoid the overloading of the PTRMS signal. Normal operation of the PTRMS is possible if the concentration of the analyzed gas does not exceed 70,000–80,000 ppb. Consequently, the absolute values of the PTRMS signals were determined by both the pressure in the gas cell and the pressure drop from the reactor to the mass spectrometer, which can differ among experiments. The value of the pressure drop (A) was determined by comparing the PTRMS signal of ethylene (C(Et)) with its partial pressure (p(Et)) measured in a reaction cell using a Baratron vacuum gauge,

$$A_i(\mathrm{Et}) = p_i(\mathrm{Et})/C_i(\mathrm{Et}), \tag{1}$$

where index i represents the various experiments. Ethylene was chosen as the calibrating gas for two reasons. First, PTRMS is sensitive to ethylene (i.e., its proton affinity is higher than that of H_3O^+); second, the PTRMS signal of ethylene was almost stable in one experiment, because of low conversion of ethylene under the reaction conditions used (see below). The latter property allowed us to check the calibration from time to time. The linearity of the dependence (1) was checked in a blank experiment by varying ethylene partial pressure from 0.02 to 0.1 mbar. The measured PTRMS signal was varied from 11,000 to about 54,000 ppb to demonstrate the quantitative correspondence of

the values of PTRMS signals and partial pressures in the reaction cell.

The PTRMS signals of ethylene oxide were recalibrated to the corresponding values of partial pressures using the following equation:

$$p_i(\mathrm{EtO}) = C_i(\mathrm{EtO})/C_i(\mathrm{Et}) \times p_i(\mathrm{Et}) = C_i(\mathrm{EtO}) \times A_i(\mathrm{Et}). \quad (2)$$

This equation suggests that ethylene oxide exhibits the same (or similar) proton affinity as ethylene. In general, the proton affinities of ethylene and ethylene oxide or their probabilities to react with H_3O^+ can differ significantly. This difference in proton affinity can be taken into account by a simple introduction to Eq. (2) of some coefficient that is equal to the ratio of proton affinities (*PA*s) and normalizes the calculated partial pressure of ethylene oxide (P_{calc}) to the real one (P_{real}), as follows:

$$P_{\mathrm{real},i}(\mathrm{EtO}) = P_{\mathrm{calc},i}(\mathrm{EtO}) \times k = P_{\mathrm{calc},i}(\mathrm{EtO}) \times PA(C_2H_4)/PA(C_2H_4O). \quad (3)$$

But this coefficient must be identical for different experiments. Then the neglect by k will result in absolute, but not relative, error. Consequently, this will not affect the comparison of the results of experiments performed under varying conditions.

The sample was a polycrystalline Ag foil (99.99% purity) mounted on a temperature-controlled heating stage. The sample was cleaned by the standard cleaning procedure: Ar^+ sputtering, annealing in 10 mbar of O_2 at 570 K, and flashing up to 800 K in vacuum [1–7]. Because of the residual gas pressure of 10^{-8} mbar in our chamber, the sample at room temperature was always covered by some hydrocarbon contaminants; however, this contamination vanished when the sample was heated to >420 K in the reaction mixture (or in pure O_2). Other impurities were not observed within the XPS sensitivity limit after the cleaning procedure. The sample temperature was measured with an alumel–chromel thermocouple attached directly to the back of the sample.

3. Results

Fig. 1 shows the PTRMS signals of ethylene and ethylene oxide recalibrated to the pressure units (see Experimental section) as a function of temperature and time. Two sets of conditions were applied in these experiments: (a) $p(C_2H_4) = 0.1$ mbar, $p(O_2) = 0.25$ mbar; and (b) $p(C_2H_4) = 0.24$ mbar, $p(O_2) = 0.25$ mbar. The last parts of the curves were measured at $T = 470$ K (a) and 520 K (b), respectively, after the oxygen flow was stopped. Although the ethylene signal does not vary for the duration of the experiment (i.e., for >5 h), the PTRMS signal from ethylene oxide increases with temperature. After the O_2 flow is stopped, the PTRMS signal of ethylene oxide decreases rapidly to the background level. These results indicate that in the millibar pressure range and at $T \geqslant 420$ K, ethylene oxide is formed as a result of ethylene epoxidation over silver. This conclusion is confirmed by data from a blank experiment showing that the temperature-controlled heating stage (heater and power wires) in the absence of the silver does not produce ethylene oxide in the temperature range investigated in our experiments (300–600 K). From Fig. 1, it is obvious that the catalytic activity of silver in the ethylene epoxidation increased with increasing catalyst temperature, as reported previously by Campbell [1,2]. From the PTRMS data, it also follows that the catalytic activity is constant at 420 K and it decreases with time

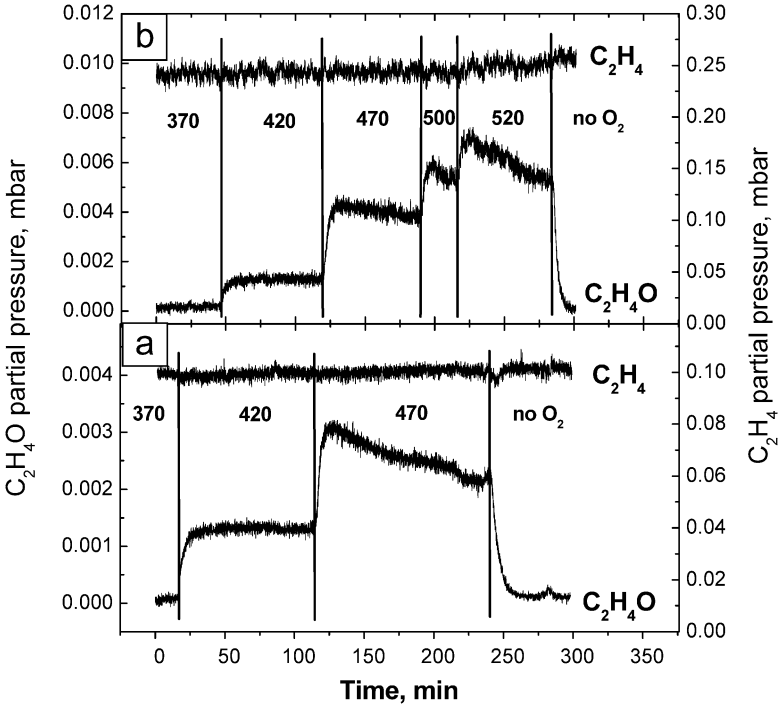

Fig. 1. Variation of the PTRMS signals from ethylene and ethylene oxide with temperature, measured in reaction mixtures of (a) $p(C_2H_4) = 0.1$ mbar, $p(O_2) = 0.25$ mbar; (b) $p(C_2H_4) = 0.24$ mbar, $p(O_2) = 0.25$ mbar. The last parts of the curves were measured after stopping the oxygen flow. PTRMS signals were converted to the partial pressures in reaction cell (see Experimental section).

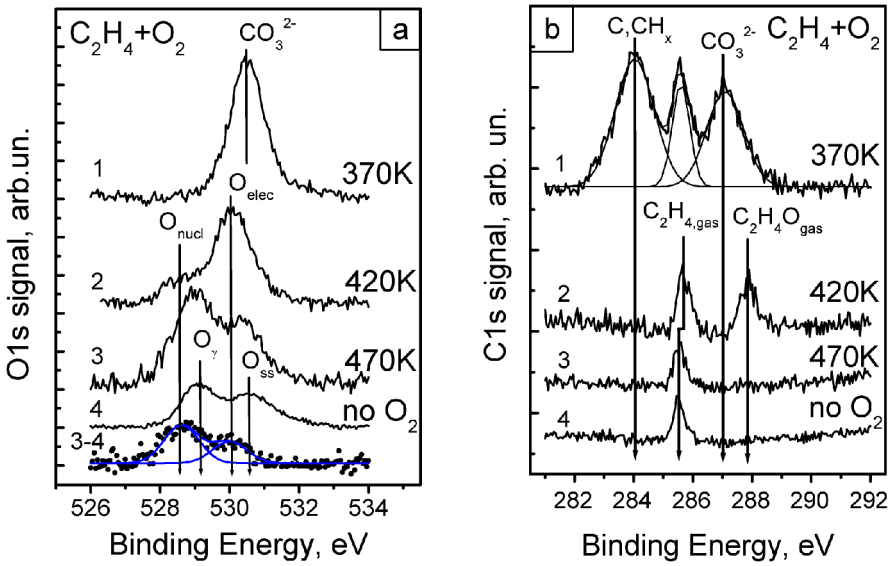

Fig. 2. O 1s (a) and C 1s (b) spectra measured in situ under the reaction mixture flow at $p(C_2H_4) = 0.1$ mbar, $p(O_2) = 0.25$ mbar and at various temperatures: 1, 370 K; 2, 420 K; 3, 470 K. Spectra 4 were measured at 470 K after the oxygen flow was stopped. The difference spectrum between the measurements in the reaction mixture and in pure ethylene (3–4) shows peaks that exist on the surface only under reaction conditions.

at 470 K and above. This observation points to deactivation of the catalyst at $T \geqslant 470$ K.

The permanency of the PTRMS signal from ethylene is due to the low conversion of ethylene to ethylene oxide in our experiments. The PTRMS signals from C_2H_4 are higher than the signals from C_2H_4O by a factor of 25–50, and therefore the variations of the ethylene pressure due to its conversion to ethylene oxide are within the noise level of the C_2H_4 signal.

Fig. 2 shows the O 1s and C 1s spectra measured in situ simultaneously with the PTRMS data in Fig. 1a [$p(C_2H_4) = 0.1$ mbar, $p(O_2) = 0.25$ mbar]. All O 1s spectra were normalized to the integrated intensity of the Ag $3d_{5/2}$ peak. The spectra change strongly with temperature. At 370 K, the silver surface was characterized by a single O 1s peak at 530.5 eV and three C 1s peaks at 284.2, 285.8, and 287.3 eV (Fig. 2, curves 1). Heating the sample to 420 K changed the spectra completely. At this temperature, the O 1s spectrum exhibited a main peak at 530.0 eV with a shoulder at about 528.5 eV, whereas the C 1s spectrum exhibited two separate narrow peaks at 285.8 and 287.9 eV (Fig. 2, curves 2). On a further temperature increase to 470 K, the C 1s peak at 287.9 eV disappeared (Fig. 2b, curve 3). The complex shape of the O 1s spectrum measured at this temperature suggests the presence of more than two peaks in this spectrum (Fig. 2a, curve 3). The O 1s spectrum measured after the O_2 flow was stopped exhibits two peaks at 529.1 and 530.6 eV (Fig. 2a, curve 4). The difference spectrum of the O 1s spectra measured at 470 K in the reaction mixture and in pure ethylene (Fig. 2a, curves 3–4) shows two O 1s peaks that are absent in the spectrum obtained in pure ethylene. These peaks have the same binding energies (528.5 and 530.0 eV) as were observed in the spectrum at 420 K.

Despite of the apparent complexity of this picture of the XPS spectra transformations, the numerous literature data [1–12,32–36] allow us to attribute all XPS signals to surface- and gas-phase species. Although gas-phase molecules do not contribute to XPS spectra under UHV conditions, at the elevated pressures of in situ experiments their concentration in the volume over the sample surface irradiated by the incident X-ray beam can become comparable with the concentration of surface species. Indeed, as we showed in previous work, measurable gas-phase XPS signals appeared in similar experiments when pressure exceeded 0.05 mbar [6,27,28]. Nonetheless, gas-phase molecules exhibit generally narrower XPS lines than surface species. This suggests that C 1s features at 285.8 and 287.9 eV originate from gas-phase species. These C 1s features can be assigned to gas-phase molecules if one takes into account the composition of the gas phase in the studied system. The signal at 285.7 eV is most likely due to gas-phase ethylene. The fact that it maintains its intensity after the oxygen flow is stopped provides more evidence in favor of this assignment. From the binding energy the other C 1s peak (287.9 eV), we can conclude that it is due to gas-phase ethylene oxide, the binding energy of which is 2 eV higher than that of gaseous ethylene [37]. This assignment requires additional discussion, because the relatively high XPS intensity attributed to C_2H_4O is in apparent contradiction to the low intensity of its PTRMS signal (Fig. 1). This contradiction between XPS and MS data can be explained by the diffusion limitations of ethylene oxide in the gas phase at 420 K. Once ethylene oxide is produced at the silver surface, it may accumulate in the volume above the sample surface where the gas phase is probed by XPS. The disappearance of this signal at 470 K can be explained by the reduction of the viscosity of the gas phase at higher temperatures, which would reduce the diffusion limitation. Because this explanation is not completely convincing, we took reference measurements with individual flows of pure ethylene oxide and other possible products loaded onto the gas cell of our spectrometer. It has been shown that only ethylene oxide exhibits similar binding energy values. Other possible products that could cause this gas-phase signal (i.e., CO and CO_2) exhibit higher binding energy values. It has been

Table 1
Assignment of the C 1s and O 1s peaks to surface species observed during ethylene epoxidation over silver. Binding energies are given in eV

Surface species	O 1s BE	C 1s BE	Temperature range of observation (K)	Refs.
Carbon contaminants	–	284.2	$T < 420$	[6]
Surface carbonates	530.5	287.3	$T < 420$	[6,31–34]
Nucleophilic oxygen	528.3	–	$T \geqslant 420$	[7,9,10,32,33]
Electrophilic oxygen	530.0	–	$T \geqslant 420$	[7,9,10,42,43]
O_γ	529.1	–	$T \geqslant 470$	[44,45]
Embedded oxygen	530.6	–	$T \geqslant 470$	[44]

also observed that acetaldehyde, often considered a main intermediate in the route of ethylene oxide combustion [3–5], is characterized by two different features in the C 1s spectrum originating from nonequivalent carbon atoms in CH_3–CH_2=O. All of these data are in full agreement with the literature [37]. XPS observation of gas-phase ethylene oxide is of great significance because it allows unambiguous identification of the PTRMS signal at $m/z = 45$ (Fig. 1) as ethylene oxide, but not as acetaldehyde. Technically, these isomers exhibit very similar mass spectra [38].

The assignments of other C 1s and O 1s features observed in our experiments are summarized in Table 1. An additional criterion reinforcing this assignment was the temperature range in which they occurred. For example, assignment of an O 1s feature at ∼530.5 eV and a C 1s feature at ∼287.5 eV observed at 370 K to surface carbonates, $CO_{3,ads}$ [6,32–35], was based not only on the binding energy values, but also on the stability on silver surfaces at ambient temperatures only. At 420 K, carbonates decompose to adsorbed oxygen and CO_2, which desorbs from the surface [6,31–34]. Consequently, the corresponding features disappear from the XPS spectra. Closeness of the O/C atomic ratio calculated from the corresponding XPS peak intensities (2.8–2.9) to the stoichiometric peak intensity (3.0) also confirms this assignment. Because of its low binding energy, the additional C 1s peak at 284.2 eV observed in the same temperature range (<420 K) can be assigned to carbonaceous residues. The accumulation of carbon-containing contaminants of different nature (e.g., graphitic carbon, hydrocarbons) on silver surfaces at ambient temperatures is also a well-known phenomenon.

The absence of C 1s features from surface species suggests that the O 1s signals observed at 420 K and above are caused by oxygen species. According to our previous investigations [7,9,10], binding energies of 528.5 and 530.0 eV are indicative of two oxygen species, nucleophilic oxygen and electrophilic oxygen, respectively. These terms were introduced by Grant and Lambert [3] to designate the nature of the interaction of oxygen with ethylene. The nucleophilic oxygen is active in the nucleophilic attack of the C–H bond as the first step in C_2H_4 combustion [3,39], whereas electrophilic oxygen participates in the electrophilic interaction with the C=C double bond of ethylene [3]. A detailed comprehensive study of the nature of these atomic oxygen species by XPS, XAES, UPS and XANES was provided in recent work [9,10]. Briefly, nucleophilic oxygen has an oxidic nature and is formed as result of silver surface reconstruction [9,10,32–35] in the course of oxygen adsorption, whereas electrophilic oxygen is adsorbed on the silver surface without reconstruction. Electrophilic oxygen was identified as adsorbed oxygen by Rocca et al. using HREELS [40,41] and by Bukhtiyarov et al. using angle-dependent XPS [42] on the basis of experiments on O_2 adsorption at Ag(100) and Ag(111) single-crystal surfaces at room temperature. King et al. also found this oxygen species as a low-coverage phase ($\Theta < 0.25$) in recent STM investigations [43,44].

The binding energy of the feature at ∼529.0 eV is close to that of the so-called "O_γ oxygen," which has been extensively studied by Schlögl et al. [45,46]. This species represents strongly bound atomic oxygen embedded in the outer layers of silver, with oxygen atoms occupying part of the silver positions in the silver crystal lattice. The peak at 530.5 eV can be assigned to subsurface oxygen embedded in octahedral holes, or O_β in our old classification [45]. The location of these oxygen species in the subsurface region is in line with its inactivity toward ethylene.

Fig. 3 shows O 1s and C 1s spectra from the polycrystalline silver foil measured in situ at 420 K, with $p(O_2) =$ 0.33 mbar and various ethylene partial pressures: 0, 0.03, 0.1, and 0.24 mbar. The figure also shows the spectra measured in UHV before the experiments in the reaction mixtures for comparison. The initial silver surface measured in UHV was free of oxygen but contained some carbonaceous residues (Fig. 3, curve 1). When oxygen was admitted to the chamber, the carbon contamination was removed, and nucleophilic oxygen (binding energy, 528.3 eV) formed on the silver surface (Fig. 3, curves 2). Introducing ethylene to the gas flow transformed the spectra. Even the smallest partial pressure of ethylene ($p(C_2H_4)/p(O_2) = 1{:}10$) reduced the O 1s signal from nucleophilic oxygen and led to the appearance of a new peak at 530.0 eV (Fig. 3a, curve 3) due to electrophilic oxygen, as discussed earlier. An increase in the partial pressure of ethylene up to $p(C_2H_4)/p(O_2) = 1{:}3$ and further to 1:1 led to a reduced surface concentration of nucleophilic oxygen and an increased coverage by electrophilic oxygen. Signals from gas-phase ethylene (285.8 eV) and ethylene oxide (287.9 eV) are observed in the C 1s spectra for all partial pressures of ethylene (Fig. 3b, curves 3–5). The intensity of the peak at a binding energy of 285.8 eV is increased with rising C_2H_4 pressure, confirming the assignment of this peak to gas-phase ethylene.

Ag $3d_{5/2}$ spectra measured simultaneously with the O 1s and C 1s spectra in Fig. 3 are shown in Fig. 4. The spectrum measured in vacuum before the experiments in the reaction mixtures is also shown (Fig. 4, curve 1). We used this spectrum for comparison with the Ag $3d_{5/2}$ spectra taken in situ; for comparison, the UHV Ag $3d_{5/2}$ spectrum is shown with open circles together with the in situ spectra. The formation of nucleophilic oxygen on the introduction of oxygen at 420 K broadened the Ag $3d_{5/2}$ spectrum compared with the spectrum taken in UHV (Fig. 4, curve 2). The difference spectrum (full circles) shows that this broadening was due to the appearance of a new feature at 367.65 eV. This feature is a clear indicator of silver ions $Ag^{\delta+}$ [7,10,43,44,47]. Using XPS signals from the nucleophilic oxygen (Fig. 3a) and from ionic silver (Fig. 4, difference spectrum),

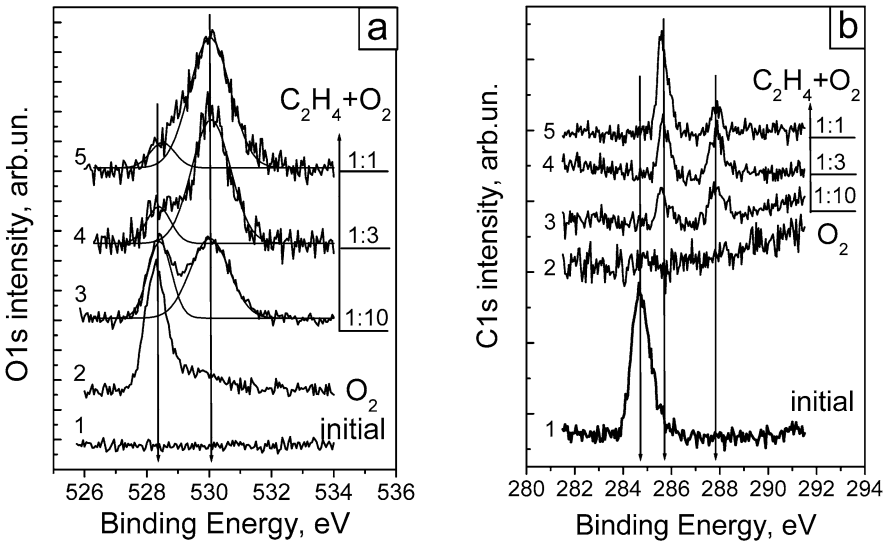

Fig. 3. O 1s (a) and C 1s (b) spectra measured in situ in the reaction mixture at 420 K, $p(O_2) = 0.33$ mbar and various $p(C_2H_4)$: 2, 0 mbar (pure O_2); 3, 0.03 mbar (1:10); 4, 0.1 mbar (1:3); 5, 0.24 mbar (1:1). The spectra from initial, "clean" silver surface measured in UHV (1) are also shown for comparison.

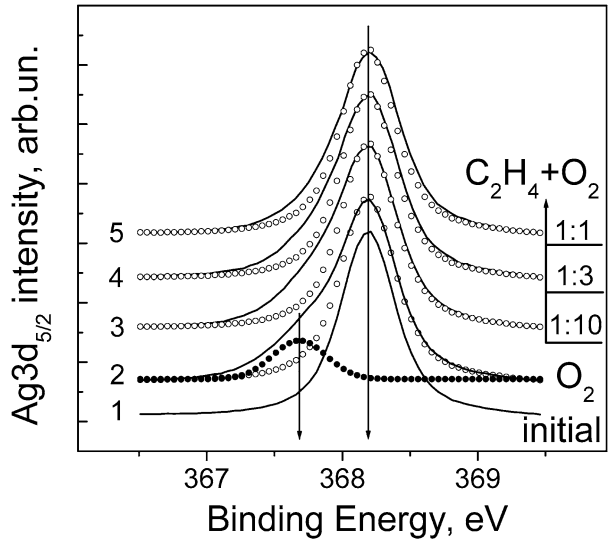

Fig. 4. Ag $3d_{5/2}$ spectra measured in situ under the reaction mixture flow at 420 K, $p(O_2) = 0.33$ mbar and various $p(C_2H_4)$: 2, 0 mbar (O_2); 3, 0.03 mbar (1:10); 4, 0.1 mbar (1:3); 5, 0.24 mbar (1:1). The spectrum measured from initial, "clean" silver surface measured in UHV is shown as curve 1. For direct comparison with the spectra measured under reaction conditions it is plotted several times as open circles. Difference spectrum (full circles) between measurements in pure O_2 (2) and in UHV (1) shows the Ag $3d_{5/2}$ component associated with nucleophilic oxygen.

we calculated the O/Ag atomic ratio, which was close to 0.5. This value indicates that one species of nucleophilic oxygen produces two silver ions, suggesting the formation of an Ag_2O surface oxide.

Adding 0.03 mbar of ethylene to the oxygen flow reduced both the O 1s intensity at 528.3 eV (Fig. 3a, curve 3) and the Ag $3d_{5/2}$ intensity at 367.6 eV (Fig. 4, curve 3), so that the O/Ag atomic ratio of the nucleophilic oxygen to ionic silver remained constant. This was also valid for the reaction mixtures with 0.1 and 0.24 mbar of ethylene (Figs. 3a and 4, curves 4 and 5). These results indicate a correlation between the amount of $Ag^{\delta+}$ ions and the concentration of nucleophilic oxygen.

4. Discussion

The results presented in the previous section show that using in situ XPS, we characterized the chemical composition of a catalytically active silver surface during ethylene epoxidation. It should be noted that similar PTRMS data have been obtained in the absence of X-rays, indicating the absence of beam-induced effects on catalytic properties of the silver. A simple comparison of the catalytic (Fig. 1a) and spectroscopic (Fig. 2) data allows us to propose a preliminary explanation for the temperature-induced variation of the catalytic properties of silver. The low activity of silver at <420 K was caused mainly by the presence of carbonates and carbonaceous residues at the silver surface, which reduced the available silver surface area for the catalytic reaction. When those contaminations were removed from the surface at 420 K, the silver surface became catalytically active for ethylene oxide formation (see Fig. 1a). The presence of nucleophilic and electrophilic oxygen at the active silver surface suggests that they participated in the ethylene oxidation reaction. Enhancement of the ethylene oxide yield at >420 K is most likely determined by the Arrhenius dependence of the reaction rate on temperature. The decreased rate of ethylene oxide formation with time observed at $\geqslant 470$ K can be explained by the accumulation of embedded oxygen species at the silver surface, which decreased the surface area available for formation of the active species. Nucleophilic and electrophilic oxygen, the main species at 420 K, were still present on the silver surface at 470 K; however, they were rapidly removed in the absence of oxygen in the gas phase (see the difference spectrum in Fig. 2a). These observations confirm the reactivity of nucleophilic and electrophilic oxygen species toward ethylene.

Elucidating the role of these species in the mechanisms of ethylene epoxidation requires a quantitative comparison of the XPS and MS data. The intensity of the corresponding O 1s peak

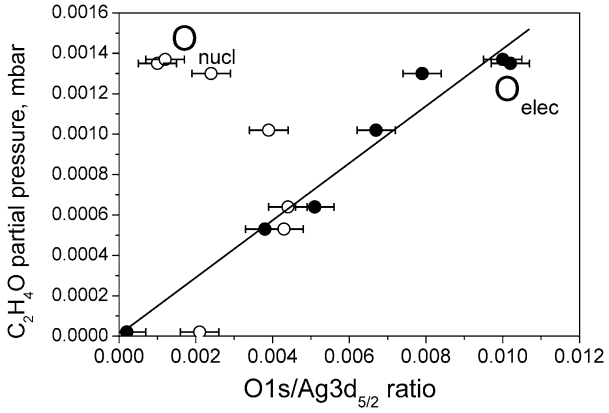

Fig. 5. The yield of ethylene oxide as a function of the abundance of the nucleophilic (open symbols) and the electrophilic (full symbols) oxygen. All measurements were performed at 420 K and at various partial pressures of oxygen and ethylene (see the text).

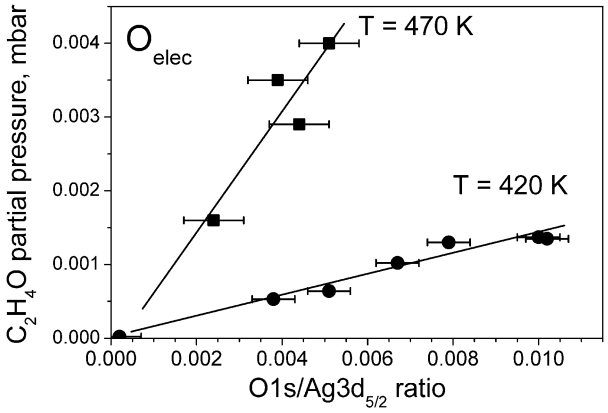

Fig. 6. The yield of ethylene oxide as a function of the abundance of the electrophilic oxygen measured at different temperatures: 420 K (circles) and 470 K (squares).

normalized to the Ag $3d_{5/2}$ intensity was used as a quantitative measure of the surface concentration of oxygen species. The normalization was necessary to take into account the effect of attenuation of the photoelectrons in the gas phase, which is quite sensitive to the pressure in the millibar range. Because the kinetic energies of Ag $3d_{5/2}$ and O 1s photoelectrons during measurement were the same (see Experimental section), so their attenuation in the gas phase should be also similar. Consequently, the O 1s/Ag $3d_{5/2}$ atomic ratios should not depend on pressure of the gas phase. The yield of ethylene oxide was expressed as partial pressure of ethylene oxide recalibrated from PTRMS signals in accordance with the procedure described in Experimental section. A comparison of the C_2H_4O yield with the abundance of nucleophilic and electrophilic oxygen for the experiments at 420 K is shown in Fig. 5. One can see a clear correlation between the abundance of the electrophilic oxygen and the yield of C_2H_4O; the higher the O 1s/Ag $3d_{5/2}$ atomic ratio for this oxygen, the higher the partial pressure of ethylene oxide. This dependence is easily approximated by a straight line aspiring to the point of origin. The resulting linear correlation can be interpreted as reflecting the participation of electrophilic oxygen in the production of ethylene oxide. This conclusion is in full agreement with the results of our previous experiments on monitoring of the isotope composition of CO_2 and C_2H_4O produced as temperature-programmed reaction (TPR) of ethylene coadsorbed with the isotopically labeled oxygen species; electrophilic oxygen was prepared with $^{16}O_2$, and nucleophilic oxygen was prepared with $^{18}O_2$ [48]. Only electrophilic oxygen labeled as ^{16}O interacted with ethylene resulting in $C_2H_4\,{}^{16}O$, whereas no signal from $C_2H_4\,{}^{18}O$ was observed in TPR spectra.

A more complicated dependence of ethylene oxide yield versus of the oxygen abundance was observed for the nucleophilic oxygen (Fig. 5). Although different ethylene oxide yields (0.0013 and $<10^{-5}$ mbar) can correspond to similar abundances of nucleophilic oxygen [I(O 1s)/I(Ag $3d_{5/2}$) ≈ 0.02], the general trend is toward a reduced yield of ethylene oxide with increasing surface concentration of nucleophilic oxygen. This result can be explained by earlier reported activity of nucleophilic oxygen in total oxidation of ethylene only. Indeed, all attempts to date to produce ethylene oxide via titration of nucleophilic oxygen with ethylene have been unsuccessful [7,33–35]. CO_2 and water were the only products of such a titration. Moreover, the aforementioned isotope experiments [48] showed that $^{18}O_{nucl}$ incorporates to $C\,{}^{18}O_2$ but not to $C_2H_4\,{}^{18}O$.

Although the presence of embedded oxygen species at 470 K reduced the accuracy of determination of concentrations of the surface species, we tried to plot the same dependence of ethylene oxide yield on an abundance of electrophilic oxygen measured at 470 K. Fig. 6 compares this dependence with that measured at 420 K. Again, a linear correlation between the catalytic properties of silver in ethylene oxide production and the abundance of electrophilic oxygen can be seen:

$$W_{\text{epox}} = A_T \times \Theta(\text{O}_{\text{elec}}), \tag{4}$$

where A_T is the coefficient of proportionality and the index T reflects the variation of A with temperature. This result provides another argument supporting our hypothesis that this oxygen species epoxidizes ethylene. Other observations from Fig. 6 included the fact that increasing temperature enhances the slope of the correlation. The ratio of the slopes determined at 470 and 420 K (A_{470}/A_{420}) is equal to 5.85.

Because the measure of the rate of ethylene epoxidation (W_{epox}) is the EtO partial pressure in the reaction cell and A is proportional to the reaction constant, so the variation of the slopes of the observed correlations with temperature can be used to estimate the activation energy of ethylene epoxidation,

$$p(\text{C}_2\text{H}_4\text{O})_{\text{Ti}} \approx k_0 \times \exp(-E_a/RT_i) \times \Theta(\text{O}_{\text{elec}})_{\text{Ti}}, \tag{5}$$

where k_0 is the pre-exponential factor and T_i is the temperature at which the dependence of ethylene oxide yield versus coverage of electrophilic oxygen is determined. Consequently, the slope of the dependence of $p(C_2H_4O)$ versus $\Theta(O_{elec})$ will be in direct proportion to $\exp(-E_a/RT)$. Then the ratio of the slopes can be expressed as

$$\frac{A_{470}}{A_{420}} = \exp\left(-E_a/R \times \left(\frac{1}{470} - \frac{1}{420}\right)\right). \tag{6}$$

This equation can be transformed for the determination of activation energy,

$$E_a = \ln(A_{470}/A_{420}) \times R \Big/ \left(\frac{1}{420} - \frac{1}{470}\right). \quad (7)$$

Using this equation and known ratio of A_{470}/A_{420}, we calculated the activation energy, which appeared to equal 14 kcal/mol.

Similar estimates of the activation energy can be made at a higher temperature range of 470–520 K. The experimental basis for this estimation is the results of the experiment for which the PTRMS signals are shown in Fig. 1b. O 1s spectra measured sequentially at 520 K reveal that a decrease in the partial pressure of ethylene oxide from 0.0069 to 0.0054 (Fig. 1b) due to deactivation is accompanied by a decrease in the abundance of the electrophilic oxygen from $I(\text{O 1s})/I(\text{Ag 3d}_{5/2}) = 0.0027$ to 0.0018. Plotting these points in the same manner as for two previous dependencies and use the point of origin as third point, we again obtain a good correlation between the ethylene oxide yield and the abundance of electrophilic oxygen. Linear anamorphosis of the 520 K dependence results in a line with a slope 3.18 times higher than the slope at 470 K. The introduction of this value of A_{520}/A_{470} to the equation

$$E_a = \ln(A_{520}/A_{470}) \times R \Big/ \left(\frac{1}{470} - \frac{1}{520}\right) \quad (8)$$

leads to an activation energy value of 11.3 kcal/mol.

Both of these values are in very good agreement with the activation energy values reported in the literature for surface science experiments on ethylene epoxidation over bulk silver samples. For example, the value of 10.8 kcal/mol was determined by Grant and Lambert as the activation energy of the epoxidation pathway for Ag(111) at 500 K [3], whereas Campbell reported 17.3 kcal/mol for the same single crystal at 440 K [2]. More detailed analysis of the activation energy of ethylene epoxidation was done by Stegelmann et al. [14] using a microkinetic model that they developed based on the results of surface science experiments. Those authors concluded that activation energy varies as a function of reaction conditions; raising the temperature and reducing the total pressure decreases the activation energy. These effects are due to an increasing number of free sites on silver surface accessible for the reaction. They calculated the variation of activation energy with temperature for high (close to industrial) and low (typical for surface science papers) pressures. Comparison of the activation energy values determined in our experiments, 58 and 47 kJ/mol, indicates good agreement with the values taken from the work of Stegelman et al. for low-pressure curves [14]: 64 kJ/mol for 450 K and 48 kJ/mol for 500 K, respectively. All of these data again indicate that electrophilic oxygen epoxidizes ethylene to ethylene oxide.

In general, many statements of the microkinetic model developed by Stegelman and coworkers [14,15,49] are in good agreement with the data obtained in the present work, which can serve as an experimental basis for the model. The main idea of Stegelman's (or that) model is that epoxidation and combustion go through a common intermediate (oxametallacycle), as was suggested by Campbell et al. [1,2] and Barteau [11,12]. Oxametallacycle, produced in reaction of ethylene and electrophilic oxygen, can branch to ethylene oxide and to acetaldehyde. In the presence of oxygen, acetaldehyde combusts rapidly to CO_2 and H_2O. CO_2 is also produced through a parallel pathway, presumably due to interaction of ethylene with nucleophilic oxygen.

Our experiments prove that the silver surface, which is active in ethylene epoxidation, actually contains two types of oxygen species, nucleophilic oxygen and electrophilic oxygen, with different O 1s binding energy values. An abundance of electrophilic oxygen [E_b(O 1s) = 530.0–530.2 eV] correlates with the yield of ethylene oxide. This result indicates unambiguously that this oxygen species epoxidizes ethylene to ethylene oxide. Unfortunately, the insensitivity of PTRMS to CO_2 prevented us from measuring the yield of CO_2 and comparing it with the abundance of electrophilic oxygen. Consequently, we could not check on the proposition that the same reaction intermediate produced as result of interaction of ethylene with electrophilic oxygen can lead to CO_2 formation.

Note, however, that our earlier isotope experiments [48] showed that $C\,^{16}O_2$ formation occurs together with $C_2H_4\,^{16}O$ formation as a result of TPR reaction of ethylene with silver surface precovered with an isotopically labeled oxygen layer, $^{18}O_{nucl}$ and $^{16}O_{elec}$. At the time of that earlier study, we could not explain this result, but it becomes easy understandable if the same reaction intermediates can provide both epoxidation and combustion of ethylene. Unfortunately, the conditions ($T > 400$ K and $P < 1$ mbar) studied in the present work do not allow us to observe any reaction intermediates, and we cannot prove the existence of oxametallacycle under the reaction conditions.

At the same time, however, we can show that nucleophilic oxygen or surface oxide (528.2–528.5 eV), which is also produced on the silver surface under the reaction conditions studied, is active in total oxidation probably via a parallel route. This means that this oxygen species, which has been studied many times in the past, has no direct connection to ethylene epoxidation. Its possible role, which we also have proposed previously [7,10,11,48], could be in the creation of $Ag^{\delta+}$ sites for the adsorption of ethylene [50], which can then react with electrophilic oxygen to ethylene oxide in the following reaction:

$$O_{elec} + C_2H_{4,ads} \rightarrow C_2H_4O. \quad (1)$$

The preferential adsorption of ethylene on $Ag^{\delta+}$ ions has been recently suggested by Bocquet et al. [51], who studied the sequential adsorption of oxygen and ethylene on Ag(111) using STM and DFT calculations. The correlation of ionic silver and the nucleophilic oxygen was also observed in our XPS experiments (see Figs. 3a and 4). This consideration suggests that nucleophilic oxygen is not involved in the epoxidation step, but simply counts the number of active sites. Stegelmann et al. [14] concluded that ethylene can adsorb on both surface oxide and metallic silver; however, they also showed that the contribution of the latter route of ethylene adsorption is much less impor-

tant in the mbar pressure range than the route in the presence of surface oxide [15].

The main discrepancy between the present work and the microkinetic model developed earlier [14,15,49] lies in the interrelation between electrophilic oxygen and nucleophilic oxygen. Stegelman et al. proposed that electrophilic oxygen adsorbs on the surface oxide, thereby competing with ethylene for the surface sites. At the same time, our experiment at 420 K (Fig. 3) demonstrated that an increase in ethylene pressure in the $C_2H_4 + O_2$ reaction mixture replaced nucleophilic oxygen with electrophilic oxygen. This result suggests that both nucleophilic and electrophilic oxygen are produced on metallic silver sites. This makes it difficult to explain which peculiarities of oxygen–silver bonding provide the formation of electrophilic oxygen. To clarify this problem, the structure of its adsorption complex must be studied using such structural methods as scanning tunneling microscopy or photoelectron diffraction. It is evident that single-crystal surfaces should be used as objects for such a study.

It should be noted, however, that this study should be performed under the reaction conditions when a mixture of ethylene with oxygen is interacted with silver. Indeed, high vacuum conditions will transform the oxygen overlayer. On the other hand, pure O_2, which has been used and continues to be used in many investigations to form oxygen overlayers, will result in the formation of nucleophilic oxygen. However, as shown in the present study, this oxygen species plays no direct role in the epoxidation of ethylene, and consequently any specification of its structure will be solely of academic interest. Moreover, the study of electrophilic oxygen, the species epoxidizing ethylene, will require in situ measurements in the mbar pressure range ($p > 0.2$–0.3 mbar). In our low-pressure experiment carried out at $p_{\text{total}} = 0.071$ mbar, electrophilic oxygen was not observed in O 1s spectra, although nucleophilic oxygen was produced in measurable abundance, $I(\text{O 1s})/I(\text{Ag 3d}_{5/2}) = 0.0021$. In full agreement with the low concentration of electrophilic oxygen (below the XPS sensitivity limit), no PTRMS signal from ethylene oxide was observed at this pressure (see the points with zero activity in Fig. 5).

5. Conclusions

We performed combined in situ XPS and PTRMS experiments of an active silver surface during the catalytic epoxidation of ethylene to ethylene oxide. Ethylene oxide was observed among the reaction products at $T \geqslant 420$ K and $p \geqslant 0.3$ mbar. The comparison of the chemical composition of the silver surface taken from in situ XPS measurements with the mass spectrometry data showed a correlation between the yield of ethylene oxide and the abundance of electrophilic oxygen characterized by $E_b(\text{O 1s}) = 530$–530.2 eV. This correlation, which was observed at both 420 and 470 K, can be explained by the participation of electrophilic oxygen in ethylene epoxidation. The second surface oxygen species, nucleophilic oxygen (528.2–528.4 eV), is active in ethylene combustion. Accumulation of other species at $T \leqslant 370$ K (carbonates, carbonaceous species) and at $T \geqslant 470$ K (embedded O_γ and O_β oxygen species) reduces the available silver surface area for the catalytic reaction and deactivates the silver catalyst.

Our experiments also show that the chemical composition of the active silver surface under reaction conditions differed from the chemical composition measured when only one reagent was present in the gas phase, or when the surface was measured under vacuum conditions. Both active oxygen species disappeared from the XPS spectra. This underlines the importance of using in situ methods to investigate the properties of active catalyst surfaces.

Acknowledgments

The authors thank the BESSY staff for help in carrying out the experiments. V.I.B. and A.I.N. gratefully acknowledge the Max-Planck-Gesellschaft for financial support during their visit to the Fritz-Haber-Institute and during the experiments conducted at BESSY.

References

[1] C.T. Campbell, M.T. Paffett, Surf. Sci. 139 (1984) 396–416.
[2] C.T. Campbell, J. Catal. 94 (1985) 436–444.
[3] R.B. Grant, R.M. Lambert, J. Catal. 92 (1985) 364–375.
[4] R.A. van Santen, C.P.M. de Groot, J. Catal. 98 (1986) 530–539.
[5] R.A. van Santen, H.P.C.E. Kuipers, Adv. Catal. 35 (1987) 265–321.
[6] A.I. Boronin, V.I. Bukhtiyarov, A.L. Vishnevskii, G.K. Boreskov, V.I. Savchenko, Surf. Sci. 201 (1988) 195–210.
[7] V.I. Bukhtiyarov, A.I. Boronin, I.P. Prosvirin, V.I. Savchenko, J. Catal. 150 (1994) 262–273.
[8] B.S. Bal'zhinimaev, Kinet. Catal. 40 (1999) 795–810.
[9] V.I. Bukhtiyarov, M. Hävecker, V.V. Kaichev, A. Knop-Gericke, R.W. Mayer, R. Schlögl, Catal. Lett. 74 (2001) 121–125.
[10] V.I. Bukhtiyarov, M. Hävecker, V.V. Kaichev, A. Knop-Gericke, R.W. Mayer, R. Schlögl, Phys. Rev. B 67 (2003) 235422.
[11] S. Linic, M.A. Barteau, J. Am. Chem. Soc. 124 (2003) 310–317.
[12] S. Linic, M.A. Barteau, J. Am. Chem. Soc. 125 (2003) 4034–4035.
[13] F.J. Williams, D.P.C. Bird, A. Palermo, A.K. Santra, R.M. Lambert, J. Am. Chem. Soc. 126 (2004) 8509–8514.
[14] C. Stegelmann, N.C. Schiødt, C.T. Campbell, P. Stoltze, J. Catal. 221 (2004) 630–649.
[15] C. Stegelmann, P. Stoltze, J. Catal. 226 (2004) 129–137.
[16] A. Knop-Gericke, M. Hävecker, Th. Schedel-Niedrig, R. Schlögl, Top. Catal. 10 (2000) 187–198.
[17] A. Knop-Gericke, M. Hävecker, Th. Schedel-Niedrig, R. Schlögl, Top. Catal. 15 (2001) 27–34.
[18] G.A. Somorjai, G. Rupprechter, J. Phys. Chem. B 103 (1999) 1623–1638.
[19] G. Rupprechter, T. Dellwig, H. Unterhalt, H.-J. Freund, Top. Catal. 15 (2001) 19–26.
[20] W.K. Kuhn, J. Szanyi, D.W. Goodman, Surf. Sci. 274 (1992) L611–L618.
[21] E. Ozensoy, D.C. Meier, D.W. Goodman, J. Phys. Chem. B 106 (2002) 9367–9371.
[22] C. Sachs, M. Hillebrand, S. Völkening, J. Wintterlin, G. Ertl, Science 293 (2001) 1635–1638.
[23] K.B. Rider, K.S. Hwang, M. Salmeron, G.A. Somorjai, J. Am. Chem. Soc. 124 (2002) 5588–5593.
[24] R.W. Joyner, M.W. Roberts, K. Yates, Surf. Sci. 87 (1979) 501–509.
[25] V.I. Bukhtiyarov, I.P. Prosvirin, E.P. Tikhomirov, V.V. Kaichev, A.M. Sorokin, V.V. Evstigneev, React. Kinet. Catal. Lett. 79 (2003) 181–188.
[26] D.F. Ogletree, H. Bluhm, G. Lebedev, C.S. Fadley, Z. Hussain, M. Salmeron, Rev. Sci. Instrum. 73 (2002) 3872–3877.
[27] H. Bluhm, M. Hävecker, A. Knop-Gericke, E. Kleimenov, R. Schlögl, D. Teschner, V.I. Bukhtiyarov, D.F. Ogletree, M. Salmeron, J. Phys. Chem. B 108 (2004) 14340–14347.
[28] E. Kleimenov, H. Bluhm, M. Hdvecker, A. Knop-Gericke, A. Pestryakov, D. Teschner, J.A. Lopez-Sanchez, J.K. Bartley, G.J. Hutchings, R. Schlögl, Surf. Sci. 575 (2005) 181–188.

[29] E. Kleimenov, PhD thesis, Technischen Universität Berlin, 2005, published online: http://edocs.tu-berlin.de/diss/2005/kleimenov_evgueni.pdf.
[30] W. Lindinger, A. Hansel, A. Jordan, Chem. Soc. Rev. 27 (1998) 347–354.
[31] K.J.S. Sawhney, F. Senf, W. Gudat, Nucl. Instrum. Meth. A 467 (2001) 466–469.
[32] M.A. Barteau, R.J. Madix, in: D.A. King, D.P. Woodruff (Eds.), The Chemical Physics of Solid Surfaces and Heterogeneous Catalysis, vol. 4, Elsevier, Amsterdam, 1982, Chapter 4.
[33] C.T. Campbell, M.T. Paffett, Surf. Sci. 143 (1984) 517–535.
[34] C.T. Campbell, Surf. Sci. 157 (1985) 43–60.
[35] C. Backx, C.P.M. de Groot, P. Biloen, W.M.H. Sachtler, Surf. Sci. 128 (1983) 81–116.
[36] S. Linic, H. Piao, K. Adib, M.A. Barteau, Angew. Chem. Int. Ed. 43 (2004) 2918–2919.
[37] K. Siegbahn, C. Nordling, G. Johansson, J. Hedman, P.F. Hedén, K. Hamrin, U. Gelius, T. Bergmark, L.O. Werme, R. Manne, Y. Baer, ESCA Applied to Free Molecules, North-Holland, Amsterdam, 1969.
[38] http://www.nist.gov/srd/nist1a.htm.
[39] R.A. van Santen, S. Moolhuysen, W.M.H. Sachtler, J. Catal. 65 (1980) 478–480.
[40] M. Rocca, L. Savio, L. Vattuone, U. Burghaus, V. Palomba, N. Novelli, F. Buatier de Mongeot, U. Valbusa, Phys. Rev. B 61 (2000) 213–227.
[41] L. Savio, L. Vattuone, M. Rocca, F. Buatier de Mongeot, G. Comelli, A. Baraldi, S. Lizzit, G. Paolucci, Surf. Sci. 506 (2002) 213–222.
[42] V.I. Bukhtiyarov, V.V. Kaichev, I.P. Prosvirin, J. Chem. Phys. 111 (1999) 2169–2175.
[43] C.I. Carlisle, D.A. King, M.-L. Bocquet, J. Cerda, P. Sautet, Phys. Rev. Lett. 84 (2000) 3899–3902.
[44] A. Michaelides, M.-L. Bocquet, P. Sautet, A. Alavi, D.A. King, Chem. Phys. Lett. 367 (2003) 344–350.
[45] X. Bao, M. Muhler, Th. Schedel-Niedrig, R. Schlögl, Phys. Rev. B 54 (1996) 2249–2262.
[46] Th. Schedel-Niedrig, X. Bao, M. Muhler, R. Schlögl, Ber. Bunsen-Ges. Phys. Chem. 101 (1997) 994–1006.
[47] L.H. Tjeng, M.B.J. Meinders, J. van Elp, G.A. Sawatzky, R.L. Johnson, Phys. Rev. B 41 (1990) 3190–3199.
[48] V.I. Bukhtiyarov, I.P. Prosvirin, R.I. Kvon, Surf. Sci. 320 (1994) L47–L50.
[49] C. Stegelmann, P. Stoltze, J. Catal. 232 (2005) 444–446.
[50] W.M.H. Sachtler, C. Backx, R.A. van Santen, Catal. Rev.-Sci. Eng. 23 (1981) 127–149.
[51] M.-L. Bocquet, P. Sautet, J. Cerda, C.I. Carlisle, M.J. Webb, D.A. King, J. Am. Chem. Soc. 125 (2003) 3119–3125.